Charge-changing cross sections for 1–25-keV H(1s) incident on a Na-vapor target

A. M. Howald, R. E. Miers, J. S. Allen, L. W. Anderson, and Chun C. Lin
Department of Physics, University of Wisconsin, Madison, Wisconsin 53706
(Received 13 September 1983)

Measurements of the charge-changing cross sections σ_{g-} and σ_{g+} are reported for 1–25-keV fast H(1s) atoms incident on a Na-vapor target. The cross section σ_{g-} falls from 3×10^{-15} cm^2 at 1 keV to 3.5×10^{-18} cm^2 at 25 keV. The cross section σ_{g+} rises from 1.1×10^{-17} cm^2 at 2 keV to 1.5×10^{-15} cm^2 at 25 keV. Measured values of the equilibrium fractions F_-^∞ and F_+^∞ for incident H^- ions are also presented.

I. INTRODUCTION

In recent years there have been many measurements made of cross sections for the reactions of hydrogen ions and atoms with various metal vapors. In addition to its intrinsic interest, this research has been spurred in part by the requirements of the magnetic fusion energy program. In this paper we report measurements of the charge-changing cross sections σ_{g-} and σ_{g+} for electron capture and stripping, respectively, for 1–25-keV ground-level H^0 atoms incident on a Na-vapor target. Previous measurements of charge-changing cross sections for neutral hydrogen incident on Na have been made by Oparin *et al.*[1] (σ_{g+} for energies from 15–60 keV), Nagata[2] (σ_{g-} 0.56–5 keV), and Anderson *et al.*[3] (σ_{g-} and σ_{g+} 30–200 keV). The results reported here are complementary to measurements made previously in this laboratory of the cross sections σ_{-0}, σ_{-+},[4] σ_{+0}, and σ_{+-},[5] and the equilibrium fractions F_-^∞, F_+^∞, and F_0^∞ (Ref. 5) in the same energy range.

II. APPARATUS

The apparatus used in this experiment is shown in Fig. 1. A H^- beam is extracted from a duoplasmatron ion source, accelerated, and focused by a gap lens and two einzel lenses. The beam is momentum analyzed by a 10° bending magnet and is collimated by two apertures 1.5 mm in diameter and 100 cm apart. Between the collimating apertures is a gas-neutralizing cell into which Ar gas is admitted. The H^- beam is stripped in the neutralizing cell to form a H^0 beam. After passing through the second collimating aperture, the H^0 beam passes between two parallel metal condenser plates. An electric field is applied between the plates. It deflects any H^- or H^+ ions out of the H^0 beam and quenches any metastable H(2s) atoms in the H^0 beam. The distance between the gas neutralizing cell and the condenser plates is such that the time of flight of a 15-keV beam is $\sim10^{-6}$ sec. This is long enough that excited hydrogen atoms with $n\leq8$ radiatively decay to either the H(1s) or H(2s) level.[6] We estimate the excited-state fraction remaining in the H^0 beam after the deflection plates to be ~0.01.[7]

After passing through the plates, the H^0 beam enters a Na-vapor target. The Na-vapor target is a stainless-steel box with an interior length of 15 cm and an interior square cross section 3.8 cm on a side. To reduce the flow of Na atoms out of the target, stainless-steel tubes 5.1 cm long and 0.64 cm i.d. are used for the entrance and exit apertures. Suspended directly beneath the target, and connected to it by a 1.8-cm-i.d. tube, is a reservoir containing liquid Na. Both the liquid Na reservoir and the Na-vapor target are heated electrically. The Na number density in the target is determined as follows. The Na atoms are lost from the target by molecular flow at a rate that depends on the conductance of the end tubes and on the density and the velocity of Na atoms in the target and hence on the temperature of the target, T_T. The net molecular flow rate of Na atoms from the reservoir into the target depends on the conductance of the tube between the reservoir and the target and on the density and the velocity of Na atoms in the target, and hence on T_T and on the densi-

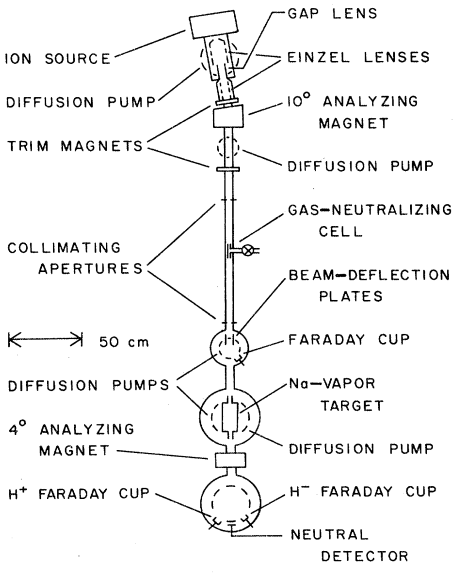

FIG 1. A schematic diagram of the apparatus.

ty and the velocity of Na atoms in the reservoir and therefore on the temperature of the reservoir, T_R. In the steady state the flow rate out of the target is equal to the flow rate from the reservoir into the target. Equating the two enables one to determine the density in the target from the various conductances and from T_T and T_R using the known vapor pressure of Na as a function of the temperature.[8] The target is kept at least 150 °C hotter than the reservoir to keep Na from condensing on it. The Na number density n is nearly constant inside the target and falls linearly to zero along the entrance and exit tubes. The target thickness π in atoms per cm^2 is therefore given by

$$\pi = n[L + \tfrac{1}{2}(L_{\text{ent}} + L_{\text{exit}})] ,$$

where L is the length of the target and L_{ent} and L_{exit} are the lengths of the entrance and exit tubes, respectively. We estimate the uncertainty in the determination of the target thickness to be $\pm 20\%$, which results primarily from uncertainty in the vapor pressure of Na as a function of temperature.

The Na metal used in this experiment was purchased in vacuum-tight glass ampules, which contain an inert atmosphere, from the Callery Chemical Company. An analysis of this Na, supplied by the manufacturer, lists K and Zn as the major impurities at 313 ppm and less than 125 ppm, respectively.[9] All other impurities account for an additional 302 ppm. The Na-vapor target, used in this experiment, has never been used with any other alkali metal. The liquid Na reservoir, used in this experiment, has been previously used with other alkali metals, but has been used only with Na during a five-year period preceding this experiment. Both target and reservoir were boiled for several hours in distilled water as the final step in the process used to clean them in preparation for this experiment.

A magnet located after the exit aperture of the Na target deflects H^+ and H^- ions, emerging from the target, into suppressed Faraday cups located at 4° on each side of the beam axis. The magnitudes of the currents measured by these Faraday cups are $I_+ = qN_+$ and $I_- = qN_-$ where q is the magnitude of the electronic charge and N_+ and N_- are, respectively, the number of positive and negative ions per second emerging from the target.

The neutral beam emerging from the target is measured by collecting the electrons ejected when the fast H^0 atoms hit a heated, polished, Cu disk. The neutral detector current is $I_0 = qN_0R(E)$, where N_0 is the number of neutral atoms per second striking the Cu disk and $R(E)$ is the average number of electrons ejected from the Cu disk per incident neutral atom. The quantity $R(E)$ depends on the energy of the incident H^0 atoms and varies from day to day as the condition of the Cu surface changes.

The currents I_+, I_-, and I_0 are measured using Keithley picoammeters. The outputs of the picoammeters are averaged for 20 sec. The apertures of each of the three particle detectors are the same size and all are located at the same distance from the target, so that each detector subtends the same angle (1.4°) as seen from the center of the target.

III. DETERMINATION OF $R(E)$

The neutral detector constant $R(E)$ is determined using an incident H^- beam. The H^- beam is produced as previously described, but with no Ar gas in the gas-neutralizing cell. The proper electric field between the beam deflection plates deflects the H^- beam into an off-axis suppressed Faraday cup before it reaches the target. The magnitude of the current measured in this cup is $I_s = qN_s$, where N_s is the number of H^- ions per second in the incident beam. After the incident beam current is measured, the deflection plates are grounded and the H^- beam enters the target where charge-changing reactions occur. The beam, emerging from the target, contains H^- ions, H^+ ions, and fast H^0 atoms. The number of particles incident on the target per second must be equal to the number of particles per second emerging from the target plus any particles lost from the beam due to scattering into angles larger than 0.7°. If the scattering losses are negligible, then

$$N_s = N_- + N_0 + N_+$$

or

$$I_s = I_- + I_0/R(E) + I_+ \tag{1}$$

or

$$I_s \cong I_- + I_0/R(E) ,$$

since in this experiment I_+ is negligible compared to either I_- or $I_0/R(E)$. As the target thickness π increases, I_- decreases and $I_0/R(E)$ increases. Equating the fall of the one to the rise of the other gives the value of $R(E)$.

In the measurement of $R(E)$, we check the assumption that scattering losses of H^- ions from the beam are small compared to the neutralization losses as follows: At very high values of π ($\pi \geq 10^{16}$ atoms per cm^2) the charge state fractions defined by

$$F_i = N_i/(N_- + N_0 + N_+);$$

where (2)

$$N_i = N_-,\ N_0,\ \text{or}\ N_+$$

become constants independent of π, but the total transmission

$$T = (N_- + N_0 + N_+)/N_s \tag{3}$$

falls exponentially as a function of π. We define a loss cross section σ_L by

$$T(\pi) = T_0 \exp(-\sigma_L \pi) . \tag{4}$$

The loss cross section σ_L must be comparable to or greater than the cross section for scattering of H^- ions into angles larger than 0.7°. For all energies in this experiment, σ_L is less than 5% of σ_{-0}, so that, in the determination of $R(E)$, loss of H^- due to scattering cannot be a major effect.

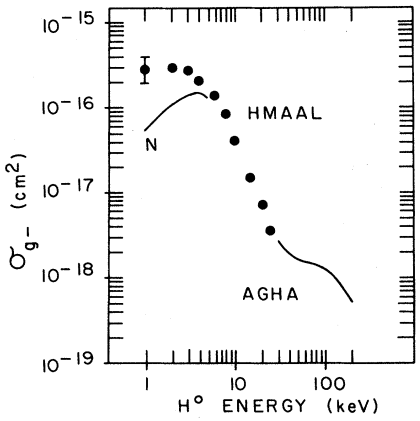

FIG. 2. Measured values of the cross section σ_{g-} as a function of H(1s) energy. HMAAL, this report; *N*, Nagata (Ref. 2); AGHA, Anderson *et al.* (Ref. 3).

IV. CROSS-SECTION MEASUREMENTS

Measurements of the charge-changing cross sections σ_{g-} and σ_{g+} are made with a beam of H^0 atoms predominently in the 1s level incident on the Na-vapor target. The beam emerging from the Na target contains H^0, H^-, and H^+. The beam currents I_0, I_-, and I_+ are measured and the charge-state fractions F_0, F_-, and F_+ are determined from Eq. (2). Clearly, $F_0+F_-+F_+=1$. For very low values of the target thickness π, and for an incident H(1s) beam, F_0, F_-, and F_+ are given by

$$F_0=1-(\sigma_{g-}+\sigma_{g+})\pi\,,$$
$$F_-=\sigma_{g-}\pi\,, \tag{5}$$

and

$$F_+=\sigma_{g+}\pi\,.$$

For low values of the target thickness π we find experimentally that the fractions F_- and F_+ increase linearly with π. The slope of F_- as a function of π is σ_{g-} and the slope of F_+ as a function of π is σ_{g+}.

The cross sections σ_{g-} and σ_{g+} are plotted as functions of incident H(1s) energy in Figs. 2 and 3, respectively. We estimate the relative uncertainty in these cross sections as functions of energy to be ±15% due primarily to uncertainty in the determination of $R(E)$ and of the slopes of F_- and F_+ as functions of π. We estimate the uncertainty in absolute values of the cross sections to be ±25%. Figures 2 and 3 also show values of σ_{g-} measured by Nagata[2] and by Anderson *et al.*[3] and of σ_{g+} measured by Oparin *et al.*[1] and by Anderson *et al.*[3] For both σ_{g-} and σ_{g+}, our measurements match up well with the higher-energy measurements of Ref. 3. Our cross section σ_{g+} is lower than that of Oparin *et al.* in the energy range in which the measurements overlap. At low energies our cross section σ_{g-} is higher than that of Nagata.

V. EQUILIBRIUM FRACTIONS

At sufficiently large values of π, the fractions F_-, F_0, and F_+ defined in Eq. (2) become constant as π increases further. The constants are called equilibrium fractions and are denoted by F_-^∞, F_0^∞, and F_+^∞. We experimentally determine these equilibrium fractions by measuring the fractions F_-, F_0, and F_+ for an incident H^- beam for very large values of π ($\pi \geq 10^{16}$ atoms per cm^2). These values of π are a factor of 2–4 times above that at which the charge composition of the beam emerging from the target is observed to stop changing, so our measurements represent the equilibrium fractions.

Before each equilibrium measurement, the apparatus is aligned at low values of π so that each beam component strikes the center of its detector. Equilibrium is reached when the target thickness is high enough that every particle in the incident beam undergoes many collisions, hence the angular spread of the H^-, H^0, and H^+ beams are all

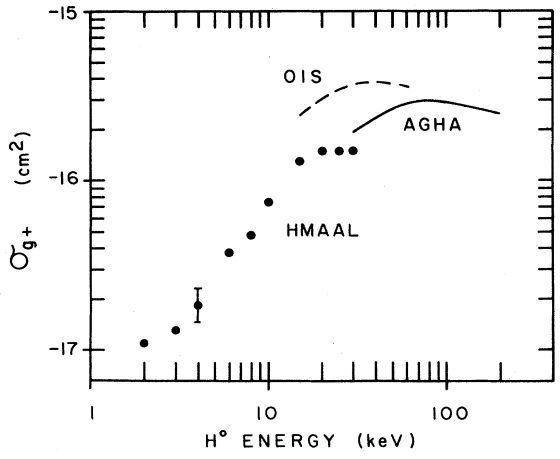

FIG. 3. Measured values of the cross section σ_{g+} as a function of H(1s) energy. HMAAL, this report; OIS, Oparin *et al.* (Ref. 1); AGHA, Anderson *et al.* (Ref. 3).

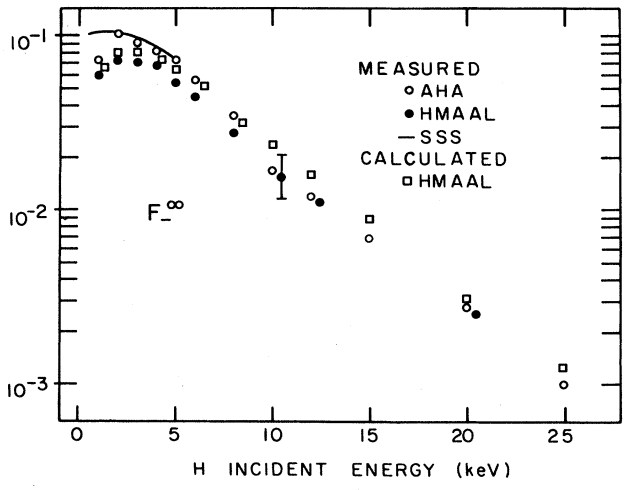

FIG. 4. Measured and calculated values of the equilibrium fraction F_-^∞. HMAAL, this report; AHA, Anderson *et al.* (Ref. 5); SSS, Schlachter *et al.* (Ref. 11).

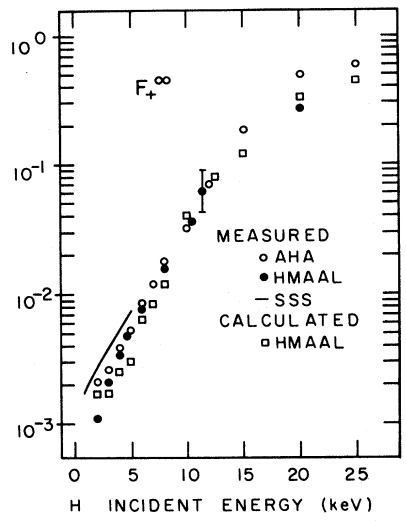

FIG. 5. Measured and calculated values of the equilibrium fraction F_+^∞. HMAAL, this report; AHA, Anderson *et al.* (Ref. 5); SSS, Schlachter *et al.* (Ref. 11).

the same.[10] Since the three detectors subtend the same angle as seen from the target, the scattering losses from the beam affect the H^-, H^0, and H^+ beam components equally. The neutral detector is calibrated as previously described.

The measured equilibrium fractions F_-^∞ and F_+^∞ are plotted as functions of energy in Figs. 4 and 5. The neutral equilibrium fraction is equal to $1-F_-^\infty-F_+^\infty$. Also shown in these figures are values of F_-^∞ and F_+^∞ measured by Schlachter *et al.*,[11] and in this laboratory by Anderson *et al.*[5] Our measurement of F_-^∞ averages about 20% lower than that of Anderson *et al.* The negative and positive equilibrium fractions of Schlachter *et al.* are also higher than ours. Our measurement was made with incident H^- ions, that of Anderson *et al.* was made with incident protons, and that of Schlachter *et al.* with incident D^+ ions, compared at the same velocity. The equilibrium fractions should be independent of the charge state of the incident ions. We do not know why our results differ from those of previous researchers. Other researchers[12–15] have measured $\eta_-^{\rm opt}$, the optimum value of the negative ion conversion efficiency η_-. The quantity η_- is defined by

$$\eta_- = N_-/N_s \ , \tag{6}$$

which differs from the definition of the negative fraction F_- given in Eq. 2 since at large values of the target density, $N_- + N_0 + N_+$ is less than N_s due to scattering losses. For this reason, values of $\eta_-^{\rm opt}$ are not directly comparable to values of F_-^∞ and are left off of Fig. 5.

If hydrogen is assumed to be a three-component system, we can write the following three coupled differential equations for F_-, F_0, and F_+:

$$\begin{aligned} dF_0/d\pi &= -F_0(\sigma_{0-}+\sigma_{0+})+F_-\sigma_{-0}+F_+\sigma_{+0} \ , \\ dF_-/d\pi &= F_0\sigma_{0-}-F_-(\sigma_{-0}+\sigma_{-+})+F_+\sigma_{+-} \ , \\ \text{and} \qquad & \qquad (7) \\ dF_+/d\pi &= F_0\sigma_{0+}-F_+(\sigma_{+0}+\sigma_{+-})+F_-\sigma_{-+} \ . \end{aligned}$$

These equations can be solved for the equilibrium fractions in terms of the six charge-changing cross sections by setting

$$dF_-/d\pi = dF_0/d\pi = dF_+/d\pi = 0 \ . \tag{8}$$

The solutions are

$$\begin{aligned} F_-^\infty &= (\sigma_{0-}\sigma_{+-}+\sigma_{0-}\sigma_{+0}+\sigma_{+-}\sigma_{0+})/D \ , \\ F_0^\infty &= (\sigma_{+0}\sigma_{-0}+\sigma_{+0}\sigma_{-+}+\sigma_{-0}\sigma_{+-})/D \ , \\ \text{and} \qquad & \qquad (9) \\ F_+^\infty &= (\sigma_{0+}\sigma_{-+}+\sigma_{0+}\sigma_{-0}+\sigma_{-+}\sigma_{0-})/D \ , \end{aligned}$$

where

$$\begin{aligned} D = {} & \sigma_{0+}\sigma_{-0}+\sigma_{0+}\sigma_{-+}+\sigma_{0+}\sigma_{+-}+\sigma_{0-}\sigma_{+-}+\sigma_{0-}\sigma_{+0} \\ & +\sigma_{0-}\sigma_{-+}+\sigma_{-0}\sigma_{+0}+\sigma_{-+}\sigma_{+0}+\sigma_{-0}\sigma_{+-} \ . \end{aligned}$$

Values of F_-^∞ and F_+^∞ calculated in this manner using our measured cross sections σ_{g+} and σ_{g-} for σ_{0+} and σ_{0-}, respectively, from this report, and the cross sections σ_{+0} and σ_{+-} from Ref. 5 and σ_{-0} and σ_{-+} from Ref. 4, are shown in Figs. 4 and 5. We believe that the agreement of the calculated and measured values of F_-^∞ and F_+^∞ is satisfactory, especially when one considers the approximations that are incorporated in using only three differential equations to analyze F_-, F_0, and F_+ as functions of π.

ACKNOWLEDGMENT

This research was supported in part by the Air Force Office of Scientific Research.

[1] V. A. Oparin, R. N. Il'in, and E. S. Solov'ev, Zh. Eksp. Teor. Fiz. 52, 369 (1967) [Sov. Phys.—JETP 25, 240 (1967)].
[2] T. Nagata, J. Phys. Soc. Jpn. 48, 2068 (1980).
[3] C. J. Anderson, R. J. Girnius, A. M. Howald, and L. W. Anderson, Phys. Rev. A 22, 822 (1980).
[4] A. M. Howald, L. W. Anderson, and C. C. Lin, Phys. Rev. A 24, 44 (1981).
[5] C. J. Anderson, A. M. Howald, and L. W. Anderson, Nucl. Instrum. Methods 165, 583 (1979).
[6] S. T. Butler and R. M. May, Phys. Rev. 137, A10 (1965).
[7] R. F. King and C. J. Latimer, J. Phys. B 12, 1477 (1979).
[8] R. Hultgreen, P. D. Desai, D. T. Hawkins, M. Gleiser, K. K. Kelley, and D. Wagman, *Selected Values of the Thermodynamic Properties of the Elements* (American Society for Metals, Cleveland, 1973).
[9] J. H. Madaus (private communication).
[10] R. J. Girnius, L. W. Anderson, and E. Staab, Nucl. Instrum. Methods 143, 505 (1977).
[11] A. S. Schlachter, K. R. Stalder, and J. W. Stearns, Phys. Rev. A 22, 2494 (1980).
[12] W. Grüebler, P. A. Schmelzbach, V. Konig, and P. Marmier, Helv. Phys. Acta 43, 254 (1970).

[13]T. Nagata, J. Phys. Soc. Jpn. 46, 919 (1979); T. Nagata (unpublished).
[14]B. A. D'yachkov, V. I. Zinenko, and M. A. Pavlii, Zh. Tekh. Fiz. 41, 2353 (1971) [Sov. Phys.—Tech. Phys. 16, 1868 (1972)].
[15]G. I. Dimov and G. V. Roslyakov, Prib. Tekh. Eksp. 3, 31 (1974) [Instrum. Exp. Tech. (USSR) 17, 658 (1974)].